HHS Public Access

Author manuscript

Acta Biomater. Author manuscript; available in PMC 2018 July 15.

Published in final edited form as:

Acta Biomater. 2017 July 15; 57: 293–303. doi:10.1016/j.actbio.2017.05.011.

Preparation and evaluation of human choroid extracellular matrix scaffolds for the study of cell replacement strategies

Kathleen R. Chirco[a,b], **Kristan S. Worthington**[a,b], **Miles J. Flamme-Wiese**[a,b], **Megan J. Riker**[a,b], **Joshua D. Andrade**[c], **Beatrix M. Ueberheide**[c,d], **Edwin M. Stone**[a,b], **Budd A. Tucker**[a,b], and **Robert F. Mullins**[a,b]

[a]The Stephen A. Wynn Institute for Vision Research, The University of Iowa, Iowa City, Iowa 52246, USA

[b]Department of Ophthalmology and Visual Sciences, The University of Iowa, Iowa City, Iowa 52246, USA

[c]Proteomics Laboratory, New York University School of Medicine, New York, New York 10016, USA

[d]Department of Biochemistry and Molecular Pharmacology, New York University School of Medicine, New York, New York 10016, USA

Abstract

Endothelial cells (ECs) of the choriocapillaris are one of the first cell types lost during age-related macular degeneration (AMD), and cell replacement therapy is currently a very promising option for patients with advanced AMD. We sought to develop a reliable method for the production of human choroidal extracellular matrix (ECM) scaffolds, which will allow for the study of choroidal EC (CEC) replacement strategies in an environment that closely resembles the native tissue. Human RPE/choroid tissue was treated sequentially with Triton X-100, SDS, and DNase to remove all native cells. While all cells were successfully removed from the tissue, collagen IV, elastin, and laminin remained, with preserved architecture of the acellular vascular tubes. The ECM scaffolds were then co-cultured with exogenous ECs to determine if the tissue can support cell growth and allow EC reintegration into the decellularized choroidal vasculature. Both monkey and human ECs took up residence in the choriocapillary tubes of the decellularized tissue. Together, these data suggest that our decellularization methods are sufficient to remove all cellular material yet gentle enough to preserve tissue structure and allow for the optimization of cell replacement strategies.

Send correspondence to: Robert F. Mullins, PhD, Stephen A. Wynn Institute for Vision Research 375 Newton Road Iowa City, IA 52242 Telephone: 319-335-8222 Robert-Mullins@uiowa.edu.

Statement of Author Contribution: KRC designed experiments, performed experiments, analyzed data, and wrote the manuscript. KSW designed experiments and edited the manuscript. MJFW, MJR, JDA, and BMU performed experiments, analyzed data, and edited the manuscript. EMS and BAT analyzed data and edited the manuscript. RFM designed experiments, analyzed data, and wrote the manuscript.

Graphical abstract

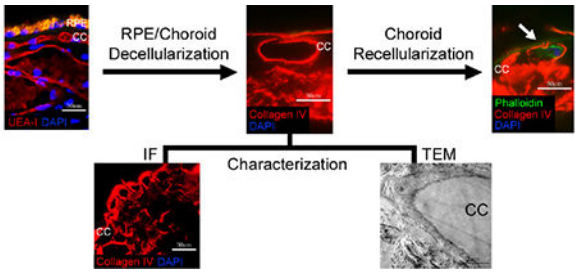

Keywords

Decellularization; choroid; choriocapillaris; extracellular matrix; age-related macular degeneration

1. Introduction

Age-related macular degeneration (AMD) is a devastating disease affecting more than 600 million people worldwide [1]. Early and intermediate AMD can be identified via funduscopic examination by the presence of drusen (extracellular material that deposits beneath the retinal pigment epithelium) and/or pigmentary changes within the macula. Advanced cases typically take on one of two forms: 1) wet AMD, in which aberrant vessels grow beneath the retinal pigment epithelium (RPE) or photoreceptor cells, forming choroidal neovascular membranes (CNVMs) within the macula, or 2) advanced dry AMD, which is characterized by regions of atrophy, termed geographic atrophy (GA), within the macula [2]. Patients with GA experience loss of photoreceptor cells, RPE cells, and endothelial cells (ECs) of the choriocapillaris. These three cell types make up three interdependent layers of the outer retina and choroid that rely on each other for survival. Therefore, loss of any one of these cell types is often followed by eventual loss of the other two [3]. This is especially true for the choriocapillaris, which provides oxygen and nutrients to the RPE and photoreceptor cells and helps eliminate waste from photoreceptor cell turnover. Despite our knowledge of the clinical features and cell types involved in AMD, a complete understanding of the molecular changes that occur during disease pathogenesis is still being pieced together.

One phenomenon that has been gaining recognition as one of the earliest events in AMD is the loss of choroidal endothelial cells (CECs), particularly within the choriocapillaris. For example, our lab has observed a trend toward decreased vascular density, along with an increased number of ghost vessels (vessels with no ECs present) in the choriocapillaris, in early AMD eyes compared to controls [4]. In addition, loss of ECs of the choriocapillaris in AMD patients is associated with the formation of drusen beneath the RPE [4]. Interestingly, the choroid becomes significantly thinner with normal aging, and this thinning is more remarkable in patients with G [5]. Proteomic studies have also shown that EC-associated proteins, such as vonWillebrand factor, are reduced in eyes with early or intermediate AMD compared to controls, while CA4 (specific to CECs in the posterior pole of the eye) protein levels are reduced in advanced AMD eyes [6]. A study assessing the human macular RPE/choroid transcriptome revealed a decrease in CEC gene expression, with an overall

preservation in RPE gene expression, in donors with early AMD compared to controls [7]. These data suggest an early loss of CECs during disease pathogenesis. Because the RPE and photoreceptor cells rely so heavily on the choriocapillaris for support, finding a way to prevent or reverse this loss is critical to understanding and treating AMD.

Unfortunately, there is currently a lack of treatment options available for AMD patients, especially those with advanced stages of dry AMD. This is also true for patients with wet AMD that experience atrophy within the macula after prolonged exposure to anti-vascular endothelial growth factor (VEGF) agents [8],[9]. Degeneration of the choriocapillaris is detrimental to the function and survival of the photoreceptor cells. Therefore, patients who have experienced loss of CECs or cells of the outer retina will require cell replacement therapies to restore, or prevent the subsequent loss of, their central vision. In order to optimize cell replacement strategies, we first need to develop a reliable and biocompatible *in vitro* system that can be used to study various therapeutic strategies before clinical testing. One way to create such a system is to generate decellularized tissue.

Tissue decellularization is a process by which cells are removed from a tissue so that only the extracellular matrix (ECM) remains. Ideally the ECM architecture and integrity will be preserved, allowing the tissue to be used as a treatment itself, or as a scaffold to study tissue composition or cell growth. To date, many tissues have been successfully decellularized, including rat heart [10], rat liver [11], rat lung [12], rat kidney [13], and mouse brain [14]. In addition, various groups have carried out decellularization of tissues in the eye, including porcine cornea for corneal grafts [15], porcine conjunctiva for tissue engineering studies [16], rabbit lacrimal glands to study lacrimal gland restoration [17], bovine retina for the production of retinal progenitor cell culture films [18], and human Bruch's membrane to study RPE cell seeding [19],[20]. In contrast, to our knowledge, methods for decellularizing the choroid for the development of CEC transplantation protocols have not been described. Here, we present a novel protocol for the successful decellularization of human RPE/choroid tissue. The decellularized tissue was critically assessed for complete cell removal, ECM protein composition, and tissue architecture. Finally, we provide evidence for reintegration of ECs within the choroid tissue scaffold.

2. Materials and Methods

2.1. Tissue Collection and Processing

After informed consent from the donor families, human donor eyes were obtained from the Iowa Lions Eye Bank (Iowa City, IA) and all experiments were performed in accordance with the Declaration of Helsinki. Tissue was collected within 8 hours after death and samples were stored at -80°C until used for experiments. For decellularization experiments, 6 mm extramacular RPE/choroid punches were used from seven different donors ranging from 78-93 years old, with no known eye disease (Table 1). In order to assess choriocapillaris ghost vessels, a 6 mm macular RPE/choroid punch was fixed for 2 hours in 4% paraformaldehyde followed by treatment with a sucrose gradient, ranging from 5% to 20% sucrose. The punch was then embedded in 20% sucrose with optimal cutting temperature (OCT) compound (2:1 v/v) [21].

2.2. RPE/Choroid Decellularization

Decellularization steps were carried out with 6 mm punches from extramacular human RPE/choroid as follows for each protocol.

Protocol 1: 5% Triton X-100 (BP151-500; Thermo Fisher Scientific, Waltham, MA) was applied for 4 hours to disrupt DNA-protein, lipid-lipid, and lipid-protein interactions without significantly altering protein structures.

Protocol 2: 5% SDS (161-0302; BioRad, Hercules, CA) + 0.1M EDTA (E57020; Research Products International, Mount Prospect, IL) was applied for 4 hours to solubilize cell and nucleic membranes, remove cellular material, and disrupt cell adhesion to the ECM.

Protocol 3: 4M urea (U20200; Research Products International) + 0.5% Nonidet P-40 (N59000; Research Products International) was applied for 4 hours to disrupt protein interactions and remove cellular material.

Protocol 4: dH_2O was applied for 1.5 hours to begin the cell lysis process and disrupt DNA-protein interactions by changing the osmolarity of the tissue; 1% Triton X-100 was applied for 3 hours to further disrupt DNA-protein, lipid-lipid, and lipid-protein interactions without significantly altering protein structures; 1× PBS was applied for 15 minutes to rinse the tissue; 1%Triton X-100 was applied for 18 hours to ensure complete disruption of DNA-protein, lipid-lipid, and lipid-protein interactions; 1× PBS was applied for 15 minutes to rinse the tissue; 0.1% SDS + 0.1M EDTA was applied for 3 hours to solubilize cell and nucleic membranes, remove cellular material, and disrupt cell adhesion to the ECM; 1× PBS was applied for 15 minutes to rinse the tissue; 10U/mL DNase I solution (EN0521; Thermo Fisher Scientific) was applied for 1 hour at 37°C to aid in the removal of any remaining DNA; 1× PBS was applied for 15 minutes to rinse the tissue; dH_2O was applied for 1.5 hours as a final rinse. All solutions contained 1% Penicillin-Streptomycin (15140122; Thermo Fisher Scientific) and all steps were carried out at room temperature with gentle shaking, unless indicated otherwise.

2.3. Bright Field Imaging

During the most efficacious decellularization process (Protocol 4), bright field images of a representative 6 mm RPE/choroid punch were captured at each step using an IX81 Olympus microscope with a 10x objective lens and a DP71 camera. During the recellularization process, representative images of RF/6A cells migrating toward the decellularized tissue were captured using the same microscope and camera setup.

2.4. Immunofluorescence

Native and decellularized human RPE/choroid punches were embedded en face in an OCT-sucrose mixture [21]. 7 μm-thick cryosections were cut from each block and used for immunohistochemical and lectin histochemical analysis. Immunofluorescence was performed as described previously [22] utilizing the following primary antibodies: rabbit polyclonal anti-collagen IV (ab6586; Abcam, Cambridge, MA), mouse monoclonal anti-laminin (2E8; DSHB, Iowa City, IA), mouse monoclonal anti-elastin (MAB2503; EMD Millipore, Temecula, CA), rabbit polyclonal anti-CD31 (ab32457; Abcam), and rabbit

polyclonal anti-VEGF (ab51745; Abcam). Biotinylated *Ulex europaeus* agglutinin-I (UEA-I; Vector Laboratories, Berlingame, CA) and biotinylated *Sambucus nigra* lectin (EBL; Vector Laboratories) were used for lectin histochemistry. Sections were then incubated with Alexa Fluor® 488-conjugated donkey anti-mouse secondary antibody (A21202; Thermo Fisher Scientific), Alexa Fluor® 546-conjugated donkey anti-rabbit secondary antibody (A10040; Thermo Fisher Scientific), Oregon Green® 488 phalloidin (O7466; Thermo Fisher Scientific), or Avidin Texas Red (A-2006; Vector Laboratories), and all sections were counterstained with 4′,6-diamidino-2-phenylindole (DAPI; Molecular Probes, Eugene, OR). Aqua-Mount® (VWR) was used to coverslip slides, and images of each section were captured using a BX-41 Olympus microscope with a 10×, 20×, or 40× objective lens and a SPOT-RT camera.

2.5. Transmission Electron Microscopy (TEM)

Transmission electron microscopy was performed as described previously [23]. Briefly, native or decellularized human RPE/choroid tissue samples were collected and allowed to sit in 1/2-strength Karnovsky fixative overnight, followed by osmium tetroxide and uranyl acetate staining.

Samples were then gradually dehydrated using increasing concentrations of acetone, infiltrated with Spurr's resin, and then cured overnight at 70°C. Blocks containing the samples were then trimmed and ultrathin sections of ~85 nm thickness were collected on formvar-coated copper slot grids. The grids were then post-stained using uranyl acetate and lead citrate, and imaged using a JEOL 1230 transmission electron microscope.

2.6. DNA Quantification

Genomic DNA was extracted from native and decellularized human RPE/choroid punches using the NucleoSpin® Tissue kit (740952.250; Macherey-Nagel Inc, Bethlehem, PA). DNA samples were then quantified using a ND-1000 Spectrophotometer (Thermo Fisher Scientific).

2.7. SDS-PAGE and Silver Staining

Total protein was extracted from native or decellularized RPE/choroid punches using the Complete Protease Inhibitor kit (Roche Diagnostic, Indianapolis, IN) with PBS and 1% Triton X-100. For each sample, an equal volume was loaded into the respective wells of a 4-20% Mini- PROTEAN TGX precast gel (BioRad). Following SDS-PAGE, the gel was stained using the Pierce™ Color Silver Stain Kit (24597; Thermo Fisher Scientific) according to the manufacturer's instructions. Total protein staining was visualized using a VersaDoc Imager (BioRad).

2.8. Sample Preparation for Mass Spectrometry

The samples were prepared for mass spectrometric analysis as previously described [24]. In brief, the native and decellularized total protein extract samples were reduced, alkylated, and loaded onto an SDS-PAGE gel to remove any detergents and LCMS incompatible reagents. The gel plugs were excised, destained, and subjected to proteolytic digestion. The gel plugs

were incubated with 300 ng of trypsin (Promega) overnight. The resulting peptides were extracted and desalted.

2.9. Mass Spectrometry

An aliquot of each sample was loaded onto an Acclaim PepMap100 C18 75 μm × 15 cm column with 3 μm bead size coupled to an EASY-Spray 75 μm × 50 cm PepMap C18 analytical HPLC column with a 2 μm bead size using the auto sampler of an EASY-nLC 1000 HPLC (Thermo Fisher Scientific) and solvent A (2% acetonitrile, 0.5% acetic acid). The peptides were eluted into a Thermo Fisher Scientific Orbitrap Elite Mass Spectrometer increasing from 2% to 30% solvent B (90% acetonitrile, 0.5% acetic acid) over 160 minutes, followed by an increase from 30% to 40% solvent B over 30 minutes and 40-100% solvent B over 10 minutes.

High resolution full MS spectra were obtained with a resolution of 60,000 at 400 m/z, an AGC target of 1e6, with a maximum ion time of 200 ms, and a scan range from 300 to 1500 m/z. Following each full MS scan, fifteen data-dependent MS/MS spectra were acquired. The MS/MS spectra were collected in the ion trap, with an AGC target of 1e4, maximum ion time of 150 ms, one microscan, 2 m/z isolation window, fixed first mass of 150m/z, and Normalized Collision Energy (NCE) of 35.

All acquired MS2 spectra were searched against a UniProt human database using Sequest within Proteome Discoverer (Thermo Fisher Scientific). The search parameters were as follows: precursor mass tolerance ±10 ppm, fragment mass tolerance ± 0.4 Da, digestion parameters trypsin allowing 2 missed cleavages, fixed modification of carbamidomethyl on cysteine, variable modification of oxidation on methionine, and variable modification of deamidation on glutamine and asparagine. The results were filtered to only include proteins identified by at least two unique peptides.

2.10. Recellularization

Decellularized RPE/choroid tissue was incubated in cell culture medium (DMEM + 1% Penicillin-Streptomycin) for 7 days, followed by a 24-hour incubation in medium supplemented with 10 ng/mL VEGF. The tissue was then placed in the center of a 35 mm-diameter cell culture dish (351008; Corning Life Science, Tewksbury, MA) and allowed to dry for 10 minutes to adhere to the dish. Once adhered, a drop of DMEM + 10% pen-strep medium was applied to the tissue to keep it moist, and the top of a 1.5 mL Eppendorf tube was placed over the tissue to form a wall. RF/6A cells or human renal glomerular endothelial cells (HRGECs) were plated in the cell culture dish at approximately 1×10^6 cells/mL, on the outside of the wall, so that the tissue and cells were physically separated. After 24 hours, the wall was removed and new media was added over both the cells and the tissue. The dish was incubated at 37°C for 7 days to allow the cells to grow into the decellularized tissue. DMEM + 5% Fetal Bovine Serum (FBS) + 1% Penicillin-Streptomycin and Endothelial Cell Culture Medium (MD-0010; iXCells

Biotechnologies, San Diego, CA) was used for RF/6A cells and HRGECs, respectively. Media was changed every other day during the 7-day incubation.

3. Results

3.1. Multi-step protocol is optimal for complete removal of cells from human RPE/choroid

Four decellularization protocols were tested for their ability to remove all cells from human RPE/choroid punches. Post-treatment fluorescence labeling demonstrates complete loss of DAPI nuclear staining in human choroid tissue for Protocol 4 (Figure 1E), while Protocols 1 through 3 (Figure 1B-D) have nuclei densities qualitatively comparable to that of the native tissue (Figure 1A). Furthermore, residual DNA was quantified for the decellularized (Protocol 4) and native tissue to further assess cell removal. DNA content for the decellularized tissue was found to be 1.2% compared to that of the native RPE/choroid, indicating that Protocol 4 can remove over 98% of native DNA. As RPE cells become detached from Bruch's membrane during Protocol 4, progressive loss of pigment can be observed throughout the tissue (Figure 2). Low levels of pigment remain after completion of the decellularization protocol, which is likely due to retention of melanin within remnants of choroidal melanocytes. All of the decellularization presented and further characterized hereafter was performed using the multi-step protocol (Protocol 4).

3.2. ECM structure remains intact after decellularization of human RPE/choroid

Because the goal of this study is to prepare scaffolds for studying and optimizing recellularization techniques, we wanted to ensure that the architecture of the tissue was preserved. After treatment, cryosections of the decellularized choroid punches were immunolabeled using antibodies directed against various ECM markers. When compared to native human RPE/choroid tissue (Figure 3A-L), the decellularized tissue has similar quantity and structure of laminin (Figure 3A′-B′), collagen type IV (Figure 3E′-F′), and elastin (Figure 3I′-J′). Removal of ECs of the choroid was confirmed by the lack of immunolabeling for CD31 (Figure 3C′-D′) and the lectin UEA-I (Figure 3G′-H′). Vascular tubes within the decellularized choriocapillaris appear to be intact and resemble the structure observed in a donor with pathologic CEC dropout in the choriocapillaris (ghost vessels [4]; Figure 4). Native human RPE/choroid and the choroid scaffolds were also analyzed at the ultrastructure level using transmission electron microscopy (TEM). In the native RPE/choroid tissue, CECs can be seen lining the inside of the choriocapillary vessels, surrounded by the CEC basement membrane. ECM proteins within the intercapillary pillars are also present (Figure 5A). After completion of the cell removal protocol, the acellular choriocapillaris exhibits preserved choriocapillary tube ultrastructure, with the CEC basement membrane and surrounding ECM remaining intact (Figure 5B). Interestingly, in donor eyes that contain drusen, these deposits persist throughout the decellularization process (Figure 4). These data suggest that our protocol can be used to generate ECM scaffolds with preserved structural integrity, providing us with a platform to optimize recellularization of the human choroid for patients with choriocapillaris degeneration.

3.3. Mass spectrometry reveals extracellular matrix protein retention

In order to obtain a comprehensive assessment of which proteins remain after decellularization, we performed SDS-PAGE followed by silver staining and, in a separate experiment, mass spectrometry, with the native and decellularized RPE/choroid tissue. Silver staining showed an overall decrease in the number of protein bands for the decellularized

tissue compared to native tissue, with a shift toward higher molecular weight species (Figure 6). The overall loss of protein is consistent with the removal of cellular material, and the larger bands most likely represent the remaining ECM proteins. Consistent with this notion, mass spectrometry revealed various ECM proteins that remain in the choroid after decellularization, including factors that support EC growth, such as collagen type IV, laminin, elastin, and perlecan (Table 2; Supplemental Table 1). Preservation of ECM/growth factor support proteins may help to provide a desirable environment for new cells to reintegrate and thrive during recellularization. Moreover, MHC class I antigens, present in the intact tissue, were not detected in the decellularized tissue (Supplemental Table 1). To identify which protein categories are significantly enriched in the decellularized tissue, mass spectrometry data was analyzed using the WEB-based GEne SeT AnaLysis Toolkit (WebGestalt; http://www.webgestalt.org/). The Benjamini-Hochberg procedure was utilized to control the false discovery rate at $p < 0.000001$. Gene ontology (GO) analysis for the identified proteins revealed 27 enriched GO categories, 14 from the biological process directed acyclic graph (DAG), two from the molecular function DAG, and 12 from the cellular component DAG. Of these, the most significantly enriched GO categories include ECM Organization, ECM Structural Constituent, Membrane Attack Complex, and Complement Activation (Table 3).

3.4. Monkey choroidal endothelial cells and primary human endothelial cells can migrate into the decellularized human choroid

Following our determination that the decellularized tissue maintains its overall structure and ECM protein composition, we sought to evaluate the ability for this scaffold to support cell integration. After decellularization, the acellular choroid scaffolds were co-cultured with monkey CECs (RF/6A cells) to determine if and where cells could re-enter the ECM scaffold. These cells were found to be viable in co-culture with the decellularized tissue, with no observed adverse effects from the decellularization treatment (Figure 7A-C). After 10 days in culture, the RF/6A cells were present within the tissue, preferentially taking up residence within the choriocapillary tubes (Figure 7D&E). Although the RF/6A cell line is commonly used to study CEC behavior, its physiological similarity to cells that may be used for transplantation is limited as it is both nonhuman and immortal. Therefore, we also wanted to assess primary human ECs in the recellularization process. Primary human renal glomerular endothelial cells (HRGECs) were chosen for their similarity to human CECs (fenestrated ECs involved in filtration). Similar to the RF/6A cells, HRGECs migrated into the decellularized choroid after 10 days in co-culture, with the majority of the cells found within the tissue settling within the choriocapillary tubes (Figure 7F&G).

4. Discussion

A number of investigators have previously used decellularization techniques to develop scaffolds to improve cell culture techniques [18], develop cell differentiation surfaces [11], and study cell replacement [10],[15]. One advantage of using decellularized tissue to study cell replacement strategies is that it provides structural and chemical features similar to that of the native tissue and that of the pathologic tissue targeted for therapy. One challenge of decellularization is that each tissue may require a slightly different strategy. For example,

Zhang *et al* recently showed that perfusion with 0.1% SDS and 1% Triton X-100 detergents, along with 0.02% trypsin/0.05% EGTA and 40 U/mL DNase/10 U/mL galactosidase enzymes, over a 28 hour period led to the successful decellularization of porcine skeletal muscle [25]. Other protocols avoid using enzymes altogether, such as a protocol presented by Caralt and colleagues, which found that use of 0.02% trypsin/0.05% EGTA and DNase was unnecessary for the perfusion decellularization of rat kidney. Instead, they utilized multiple treatments with 1% Triton X-100 followed by 0.1% SDS [26]. With the requirement to optimize a decellularization protocol based on tissue type in mind, we developed and critically assessed a novel technique to decellularize human RPE/choroid. We have shown that our multi-step protocol, in which relatively low levels of Triton X-100 and SDS detergents are used in addition to DNase treatment, can successfully eliminate all evidence of cellular components from the tissue, while preserving ECM protein structure. Furthermore, exogenous ECs can migrate toward and take up residence within the acellular choroid scaffold, preferentially seeking out the empty vessels of the choriocapillaris. This pilot study provides us with an *ex vivo* 3D culture system to study recellularization of the choriocapillaris to bring us a step closer to our goal of rebuilding the choroid in patients with AMD.

Further studies of decellularized human choroids could be used to provide new insights about ECM composition within the choroid and about ECM interactions with AMD-associated proteins (e.g., complement factor H). Furthermore, future work could utilize this protocol to decellularize RPE/choroid tissue from AMD eyes to directly assess differences in protein composition, ECM- protein interactions, as well as cell replacement capabilities compared to control eyes.

Although we have developed a scaffold that can support cell migration and integration, further optimization will be required to gain a more complete recellularization of the tissue. For example, both insoluble ECM proteins and soluble growth factors have been shown to be important for CEC differentiation and survival. While our mass spectrometry data show the presence of ECM proteins, the tissue does not contain valuable growth factors. Some of the most important factors include VEGF, pigment epithelium-derived factor (PEDF), and basic fibroblast growth factor (bFGF) [27],[28]. VEGF and bFGF are both pro-angiogenic factors, while PEDF is anti-angiogenic [29]. The balance between pro- and anti-angiogenic factors in the choriocapillaris is critical for the preservation of a healthy environment for ECs [27]. In addition,

IGF-1 has been shown to stimulate proliferation and migration, and promote vessel formation when introduced to endothelial progenitor cells [30],[31]. In the current study we utilized exogenous VEGF to help promote EC migration toward the choroid scaffolds. Future studies will focus on determining which combination of these factors is required for optimal recellularization of the choroid with CECs, with the goal of employing these factors to supplement the ECM scaffolds.

In addition to optimizing the microenvironment for cellular integration, another key consideration of cell replacement therapy in patients is whether allogenic or autologous cells are required. Endothelial cells of the choriocapillaris, and to a lesser extent ECs of larger

choroidal vessels and the basal RPE, express high levels of human leukocyte antigen (HLA) class I molecules [32],[33]. The presence of this immune system regulatory factor in the RPE and choroid demonstrates the continuous display of self-identity to the immune system and, consequently, the need to use HLA-matched cells for replacement in patients. The most feasible way to ensure that cells are HLA-matched is to use cells originating from the patient for whom they are intended. To accomplish this, patient-specific induced pluripotent stem cells (iPSC), and in turn iPSC-derived progeny, could be used.

While this pilot study provides us with a robust decellularization protocol and demonstrates successful recellularization with ECs, there are some limitations to this work. First, due to the practical aspects of tissue collection and storage, the human tissue is flash frozen and subsequently stored at −80°C immediately following collection and prior to decellularization.

The freezing process is used to preserve proteins, RNA, DNA, and other molecules for later analyses. In addition, freezing of human tissue kills endogenous cells, which may confound the results of the decellularization experiments. However, we have observed excellent preservation of cells and tissue at the immunofluorescence and ultrastructural levels in the native RPE/choroid, even after freezing, suggesting that the freezing process itself does not significantly contribute to the removal of cells in our decellularized human RPE/choroid (Figure 5A). The second limitation of this work is the cell types used to assess recellularization of the tissue scaffold. Here, we utilized a monkey CEC line and primary HRGECs, both of which exhibit anatomical and gene expression differences from endogenous human CECs. Therefore, although this procedure allowed effective recolonization of two independent EC lines, the techniques required to recellularize the tissue may differ slightly for human CECs, and future work will utilize human iPSC-derived CECs for recellularization studies. Finally, while it was beyond the scope of the work presented here, assessing the fate of the cells that enter the tissue will be extremely important for future experiments. Once the recellularization technique has been optimized, future work will aim to fully characterize both the cells that enter and repopulate the choriocapillaris vascular tubes, as well as the cells that that enter the tissue but fail to find any vascular openings.

In summary, since CECs are lost early in the pathogenesis of AMD, developing a procedure to replace these cells is critical. Furthermore, because the choriocapillaris provides oxygen and nutrients for both the RPE and photoreceptor cells, cell replacement strategies for either of these cell types should take the health of CECs into consideration. To date, we have successfully generated CECs with iPSCs derived from mouse fibroblasts [34] and are adapting these methods toward the development of EC progenitors and CECs using human fibroblast-derived iPSCs. Using this iPSC technology in combination with our decellularization protocol, we can evaluate and optimize methods for rebuilding the choroid using iPSC-induced CECs or EC progenitors. In patients with advanced GA, in which CECs, RPE cells, and photoreceptor cells have all degenerated, it may be necessary to rebuild all three layers *in vitro* and transplant them into the macula as a single piece. Furthermore, it may be necessary to consider ECM repair in any transplantation models, as the matrix acquires age- and disease-associated changes as well [35]. The work presented here

represents a pilot study that will help guide us toward the development of effective iPSC-based replacement therapies, regardless of whether they are single- or multicell strategies.

Supplementary Material

Refer to Web version on PubMed Central for supplementary material.

Acknowledgments

We would like to thank the Iowa Lions Eye Bank and the donors and their families for their invaluable contributions to this work. This work was supported by NIH grant EY024605, the Elmer and Sylvia Sramek Charitable Foundation, Research to Prevent Blindness, and the Carver Chair in Ocular Cell Biology.

References

1. Wong WL, Su X, Li X, Cheung CMG, Klein R, Cheng CY, Wong TY. Global prevalence of age-related macular degeneration and disease burden projection for 2020 and 2040: a systematic review and meta-analysis. The Lancet Global Health. 2014; 2:e106–e116. DOI: 10.1016/S2214-109X(13)70145-1 [PubMed: 25104651]
2. Bird AC, Bressler NM, Bressler SB, Chisholm IH, Coscas G, Davis MD, de Jong PTVM, Klaver CCW, Klein BEK, Klein R, Mitchell P, Sarks JP, Sarks SH, Soubrane G, Taylor HR, Vingerling JR. An International Classification and Grading System for Age-related Maculopathy and Age-related Macular Degeneration. Surv Ophthalmol. 1995; 39:367–374. [PubMed: 7604360]
3. Korte GE, Reppucci V, Henkind P. RPE destruction causes choriocapillary atrophy, Invest. Ophthalmol Vis Sci. 1984; 25:1135–1145.
4. Mullins RF, Johnson MN, Faidley EA, Skeie JM, Huang J. Choriocapillaris Vascular Dropout Related to Density of Drusen in Human Eyes with Early Age-Related Macular Degeneration. InvestOphthalmol Vis Sci. 2011; 52:1606–1612. DOI: 10.1167/iovs.10-6476
5. Sohn EH, Khanna A, Tucker BA, Abràmoff MD, Stone EM, Mullins RF. Structural and Biochemical Analyses of Choroidal Thickness in Human Donor EyesAnalyses of Choroidal Thickness in Human Donor Eyes. Invest Ophthalmol Vis Sci. 2014; 55:1352–1360. DOI: 10.1167/iovs.13-13754 [PubMed: 24519422]
6. Yuan X, Gu X, Crabb JS, Yue X, Shadrach K, Hollyfield JG, Crabb JW. Quantitative proteomics: comparison of the macular Bruch membrane/choroid complex from age-related macular degeneration and normal eyes. Mol Cell Proteomics. 2010; 9:1031–1046. DOI: 10.1074/mcp.M900523-MCP200 [PubMed: 20177130]
7. Whitmore SS, Braun TA, Skeie JM, Haas CM, Sohn EH, Stone EM, Scheetz TE, Mullins RF. Altered gene expression in dry age-related macular degeneration suggests early loss of choroidal endothelial cells. Mol Vis. 2013; 19:2274–2297. [PubMed: 24265543]
8. Folk JC, Stone EM. Ranibizumab therapy for neovascular age-related macular degeneration. N Engl J Med. 2010; 363:1648–1655. DOI: 10.1056/NEJMct1000495 [PubMed: 20961248]
9. Young M, Chui L, Fallah N, Or C, Merkur AB, Kirker AW, Albiani DA, Forooghian F. Exacerbation of choroidal and retinal pigment epithelial atrophy after antivascular endothelial growth factor treatment in neovascular age-related macular degeneration. Retina (Philadelphia, Pa). 2014; 34:1308–1315. DOI: 10.1097/IAE.0000000000000081
10. Ott HC, Matthiesen TS, Goh SK, Black LD, Kren SM, Netoff TI, Taylor DA. Perfusion-decellularized matrix: using nature's platform to engineer a bioartificial heart. Nat Med. 2008; 14:213–221. DOI: 10.1038/nm1684 [PubMed: 18193059]
11. Zhang Y, He Y, Bharadwaj S, Hammam N, Carnagey K, Myers R, Atala A, Van Dyke M. Tissue-specific extracellular matrix coatings for the promotion of cell proliferation and maintenance of cell phenotype. Biomaterials. 2009; 30:4021–4028. DOI: 10.1016/j.biomaterials.2009.04.005 [PubMed: 19410290]

12. Ott HC, Clippinger B, Conrad C, Schuetz C, Pomerantseva I, Ikonomou L, Kotton D, Vacanti JP. Regeneration and orthotopic transplantation of a bioartificial lung. Nat Med. 2010; 16:927–933. DOI: 10.1038/nm.2193 [PubMed: 20628374]

13. Song JJ, Guyette JP, Gilpin SE, Gonzalez G, Vacanti JP, Ott HC. Regeneration and experimental orthotopic transplantation of a bioengineered kidney. Nat Med. 2013; 19:646–651. DOI: 10.1038/nm.3154 [PubMed: 23584091]

14. De Waele J, Reekmans K, Daans J, Goossens H, Berneman Z, Ponsaerts P. 3D culture of murine neural stem cells on decellularized mouse brain sections. Biomaterials. 2015; 41:122–131. DOI: 10.1016/j.biomaterials.2014.11.025 [PubMed: 25522971]

15. Luo H, Lu Y, Wu T, Zhang M, Zhang Y, Jin Y. Construction of tissue-engineered cornea composed of amniotic epithelial cells and acellular porcine cornea for treating corneal alkali burn. Biomaterials. 2013; 34:6748–6759. DOI: 10.1016/j.biomaterials.2013.05.045 [PubMed: 23764112]

16. Zhao H, Qu M, Wang Y, Wang Z, Shi W. Xenogeneic acellular conjunctiva matrix as a scaffold of tissue-engineered corneal epithelium. PLoS ONE. 2014; 9:e111846.doi: 10.1371/journal.pone.0111846 [PubMed: 25375996]

17. Lin H, Sun G, He H, Botsford B, Li M, Elisseeff JH, Yiu SC. Three-Dimensional Culture of Functional Adult Rabbit Lacrimal Gland Epithelial Cells on Decell ularized Scaffold. Tissue Eng Part A. 2016; 22:65–74. DOI: 10.1089/ten.TEA.2015.0286 [PubMed: 26414959]

18. Kundu J, Michaelson A, Talbot K, Baranov P, Young MJ, Carrier RL. Decellularized retinal matrix: Natural platforms for human retinal progenitor cell culture. Acta Biomater. 31(2016):61–70. DOI: 10.1016/j.actbio.2015.11.028

19. Tezel TH, Kaplan HJ, Del Priore LV. Fate of human retinal pigment epithelial cells seeded onto layers of human Bruch's membrane. Invest Ophthalmol Vis Sci. 1999; 40:467–476. [PubMed: 9950607]

20. Tezel TH, Del Priore LV, Kaplan HJ. Reengineering of aged Bruch's membrane to enhance retinal pigment epithelium repopulation. InvestOphthalmol Vis Sci. 2004; 45:3337–3348. DOI: 10.1167/iovs.04-0193

21. Barthel LK, Raymond PA. Improved method for obtaining 3-microns cryosections for immunocytochemistry. J Histochem Cytochem. 1990; 38:1383–1388. [PubMed: 2201738]

22. Chirco KR, Whitmore SS, Wang K, Potempa LA, Halder JA, Stone EM, Tucker BA, Mullins RF. Monomeric CDreactive protein and inflammation in ageDrelated macular degeneration. Journal of Pathology. 2016; 240:173–183. DOI: 10.1002/path.4766 [PubMed: 27376713]

23. Schubert C, Pryds A, Zeng S, Xie Y, Freund KB, Spaide RF, Merriam JC, Barbazetto I, Slakter JS, Chang S, Munch IC, Drack AV, Hernandez J, Yzer S, Merriam JE, Linneberg A, Larsen M, Yannuzzi LA, Mullins RF, Allikmets R. Cadherin 5 is regulated by corticosteroids and associated with central serous chorioretinopathy. Hum Mutat. 2014; 35:859–867. DOI: 10.1002/humu.22551 [PubMed: 24665005]

24. Cotto-Rios XM, Békés M, Chapman J, Ueberheide B, Huang TT. Deubiquitinases as a signaling target of oxidative stress. Cell Rep. 2012; 2:1475–1484. DOI: 10.1016/j.celrep.2012.11.011 [PubMed: 23219552]

25. Zhang J, Hu ZQ, Turner NJ, Teng SF, Cheng WY, Zhou HY, Zhang L, Hu HW, Wang Q, Badylak SF. Perfusion-decellularized skeletal muscle as a three-dimensional scaffold with a vascular network template. Biomaterials. 2016; 89:114–126. DOI: 10.1016/j.biomaterials.2016.02.040 [PubMed: 26963901]

26. Caralt M, Uzarski JS, Iacob S, Obergfell KP, Berg N, Bijonowski BM, Kiefer KM, Ward HH, Wandinger-Ness A, Miller WM, Zhang ZJ, Abecassis MM, Wertheim JA. Optimization and critical evaluation of decellularization strategies to develop renal extracellular matrix scaffolds as biological templates for organ engineering and transplantation. Am J Transplant. 2015; 15:64–75. doi:10.1111/ajt. 12999. [PubMed: 25403742]

27. Bhutto IA, McLeod DS, Hasegawa T, Kim SY, Merges C, Tong P, Lutty GA. Pigment epithelium-derived factor (PEDF) and vascular endothelial growth factor (VEGF) in aged human choroid and eyes with age-related macular degeneration. Experimental Eye Research. 2006; 82:99–110. DOI: 10.1016/j.exer.2005.05.007 [PubMed: 16019000]

28. Liu X, Ye X, Yanoff M, Li W. Extracellular matrix of retinal pigment epithelium regulates choriocapillaris endothelial survival in vitro. Experimental Eye Research. 1997; 65:117–126. DOI: 10.1006/exer.1997.0317 [PubMed: 9237872]

29. Dawson DW, Volpert OV, Gillis P, Crawford SE, Xu H, Benedict W, Bouck NP. Pigment epithelium-derived factor: a potent inhibitor of angiogenesis. Science. 1999; 285:245–248. [PubMed: 10398599]

30. Thum T, Hoeber S, Froese S, Klink I, Stichtenoth DO, Galuppo P, Jakob M, Tsikas D, Anker SD, Poole-Wilson PA, Borlak J, Ertl G, Bauersachs J. Age-Dependent Impairment of Endothelial Progenitor Cells Is Corrected by Growth Hormone Mediated Increase of Insulin-Like Growth Factor-1. Circ Res. 2007; 100:434–443. DOI: 10.1161/01.RES.0000257912.78915.af [PubMed: 17234973]

31. Kamprom W, Kheolamai P, U-Pratya Y, Supokawej A, Wattanapanitch M, Laowtammathron C, Issaragrisil S. Effects of mesenchymal stem cell-derived cytokines on the functional properties of endothelial progenitor cells. European Journal of Cell Biology. 2016; 95:153–163. DOI: 10.1016/j.ejcb.2016.02.001 [PubMed: 26899034]

32. Abi-Hanna D, Wakefield D, Watkins S. HLA ANTIGENS IN OCULAR TISSUES: I. in Vivo Expression in Human Eyes. Transplantation. 1988; 45:610. [PubMed: 3347938]

33. Goverdhan SV, Howell MW, Mullins RF, Osmond C, Hodgkins PR, Self J, Avery K, Lotery AJ. Association of HLA Class I and Class II Polymorphisms with Age-Related Macular Degeneration. InvestOphthalmol Vis Sci. 2005; 46:1726–9. DOI: 10.1167/iovs.04-0928

34. Songstad AE, Wiley LA, Duong K, Kaalberg E, Flamme-Wiese MJ, Cranston CM, Riker MJ, Levasseur D, Stone EM, Mullins RF, Tucker BA. Generating iPSC- Derived Choroidal Endothelial Cells to Study Age-Related Macular Degeneration iPSC- Derived Choroidal Endothelial Cells. InvestOphthalmol Vis Sci. 2015; 56:8258–8267. DOI: 10.1167/iovs.15-17073

35. Chirco KR, Sohn EH, Stone EM, Tucker BA, Mullins RF. Structural and molecular changes in the aging choroid: implications for age-related macular degeneration. Eye. 2016; doi: 10.1038/eye.2016.216

Statement of Significance

Age-related macular degeneration (AMD) is a devastating disease affecting more than 600 million people worldwide. Endothelial cells of the choriocapillaris (CECs) are among the first cell types lost in early AMD, and cell replacement therapy is currently the most promising option for restoring vision in patients with advanced AMD. In order to study CEC replacement strategies we have generated a 3D choroid scaffold using a novel decellularization method in human RPE/choroid tissue. To our knowledge, this is the first report describing decellularization of human RPE/choroid, as well as recellularization of a choroid scaffold with CECs. This work will aid in our development and optimization of cell replacement strategies using a tissue scaffold that is similar to the in vivo environment.

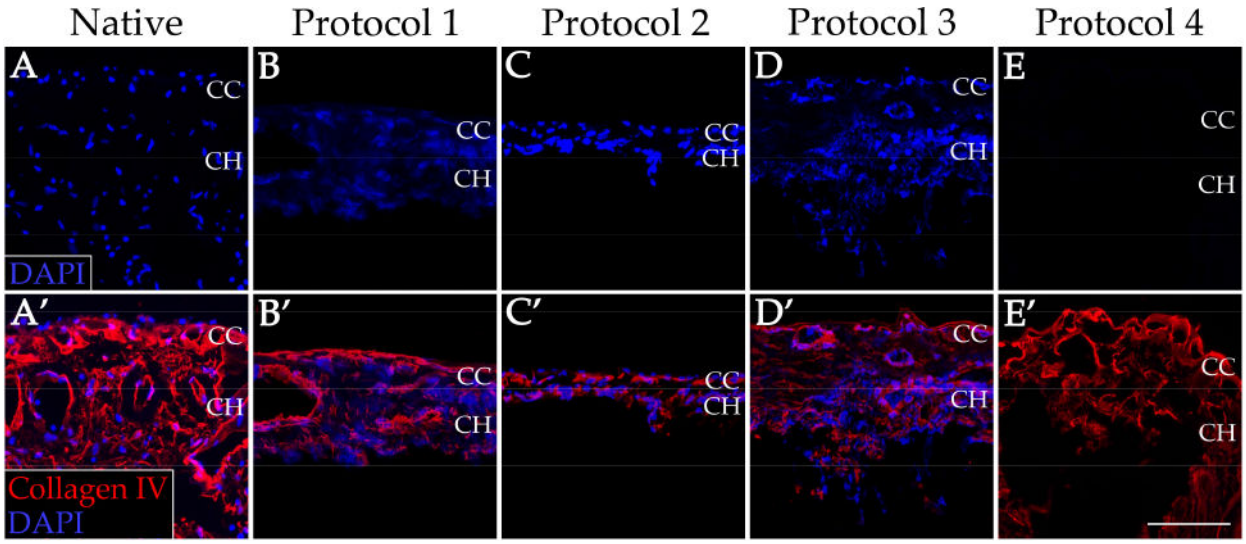

Figure 1.

Immunofluorescence staining of human RPE/choroid before and after decellularization. Cellularity, as indicated by intact nuclei (blue), and collagen IV (red) structure of the native RPE/choroid tissue (A&A') was compared to that of the tissue after four separate decellularization protocols (B-E&B'-E'). CC = choriocapillaris; CH = choroid. Scale bar = 100 μm.

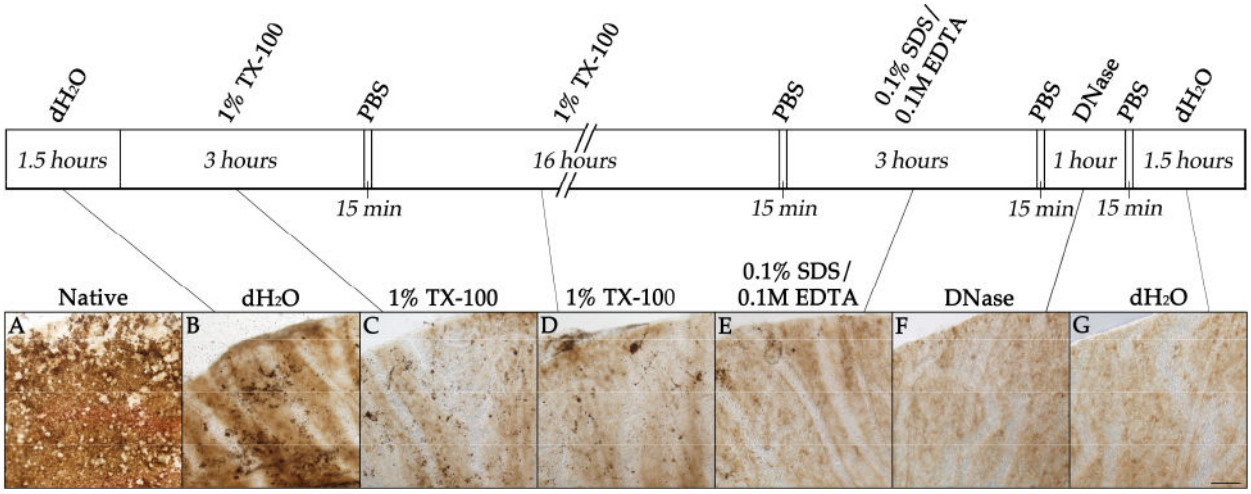

Figure 2.

Brightfield images showing human RPE/choroid at each step of the decellularization using Protocol 4. Images show the native RPE/choroid tissue (A) after sequential treatments with deionized water (B), 1% Triton X-100 (C), 1% Triton X-100 (D), 0.1% SDS + 0.1M EDTA (E), DNase I solution (F), and deionized water (G). Loss of the cobblestone appearance of the RPE pigment can be observed, while minor amounts of choroidal melanin remain. Scale bar = 200 lμm.

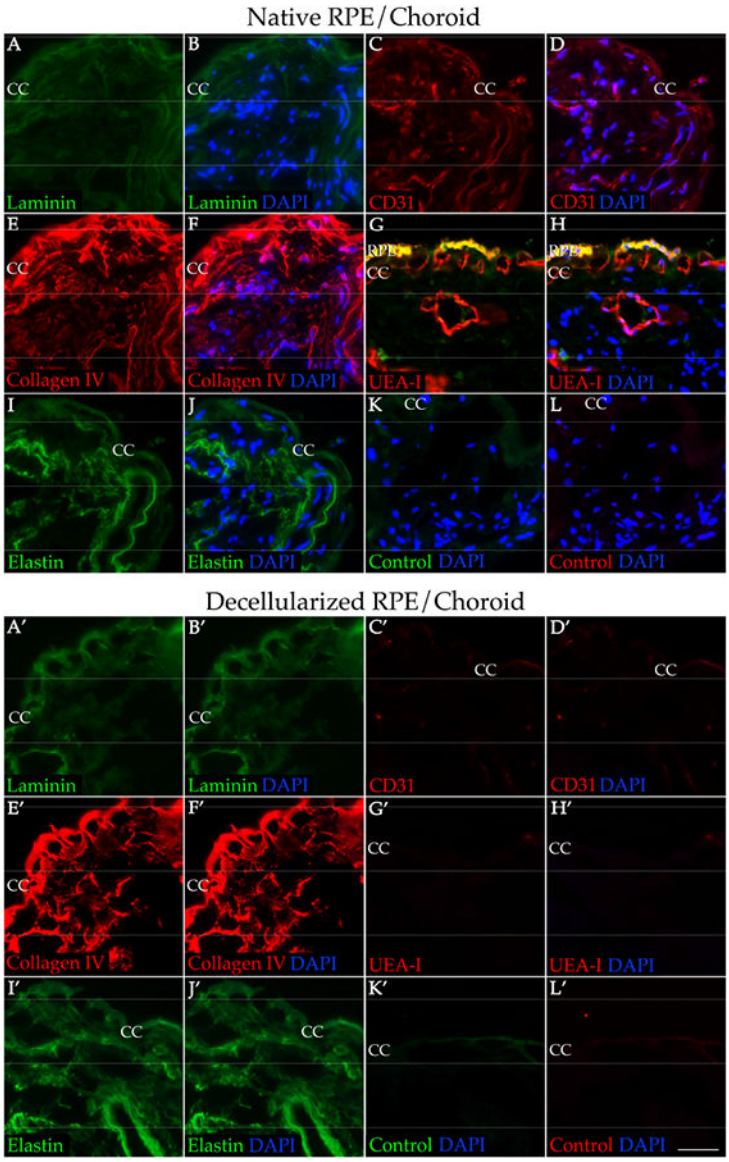

Figure 3.

Preservation of key ECM proteins and loss of EC markers in decellularized human RPE/choroid compared to native tissue. Native RPE/choroid (A-L) and decellularized RPE/choroid (A′-L′) were immunolabeled with antibodies against laminin (A-B&A′-B′; green), collagen IV (E-F&E′-F′; red), elastin (I-J&I′-J′; green), CD31 (C-D&C′-D′; red), and UEA-I (G-H&G′-H′; red). K-L & K′-L′ were labeling with secondary antibody only. All sections were counterstained with DAPI (B&B′, D&D′, F&F′, H&H′, J&J′, K&K′, L&L′; blue). RPE = retinal pigment epithelium; CC = choriocapillaris. Scale bar = 50 μm.

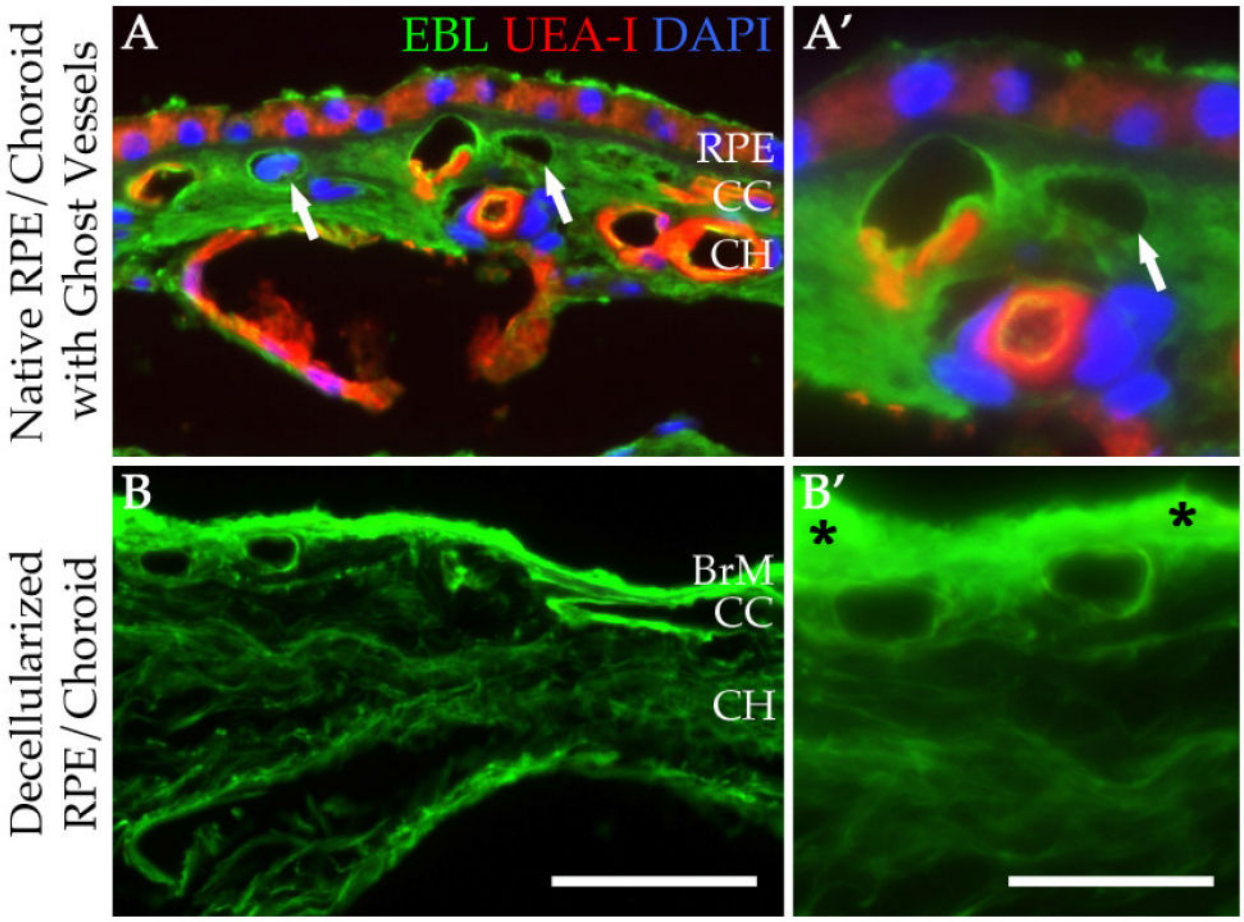

Figure 4.

Structural similarity between human RPE/choroid with ghost vessels and decellularized tissue. Native RPE/choroid (A&A′) and decellularized RPE/choroid (B&B′) were labeled with EBL (green) and UEA-I (red) lectins. Sections were counterstained with DAPI (blue). Drusen deposits were retained throughout the decellularization process (B′, asterisks). Arrows (A&A′) indicate ghost vessels. RPE = retinal pigment epithelium; CC = choriocapillaris; CH = choroid. Scale bar in B = 50 μm; scale bar in B′ = 25 μm.

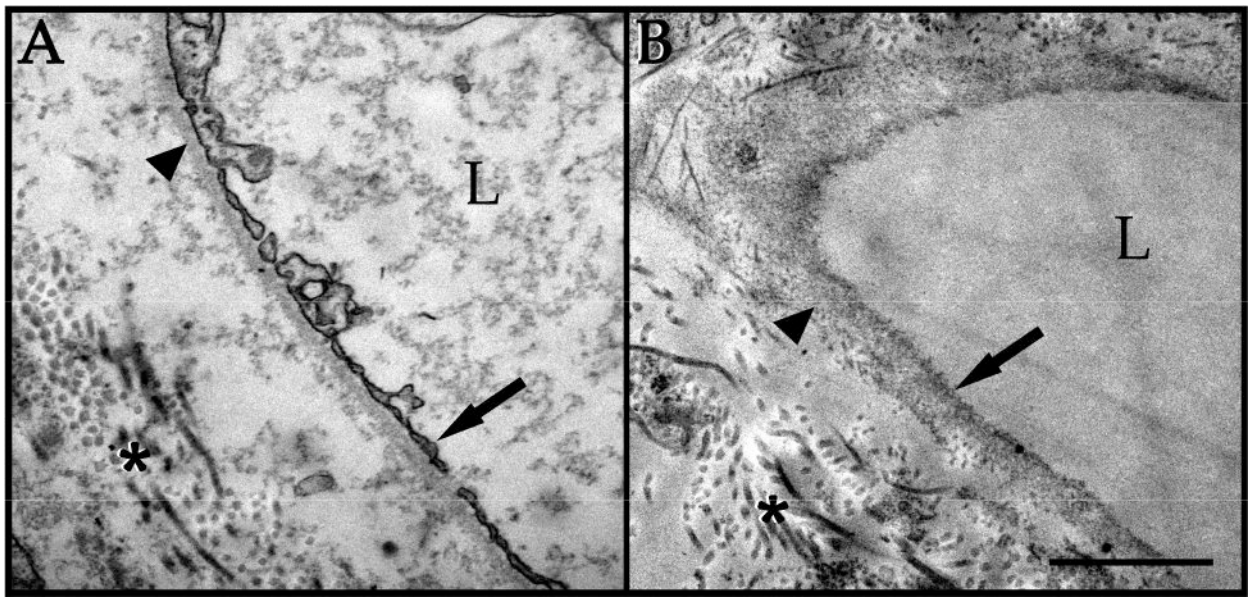

Figure 5.

TEM confirmation of ECM/basement membrane preservation and cell loss in decellularized human RPE/choroid. Native choriocapillaris (A) exhibits endothelial cells lining the choriocapillary vessels (arrow), surrounded by basement membrane (arrowhead) and ECM (asterisk). Decellularized choriocapillaris (B) shows loss of CECs (arrow), with preserved basement membrane (arrowhead) and ECM (asterisk). L = vascular lumen. Scale bar = 1 μm.

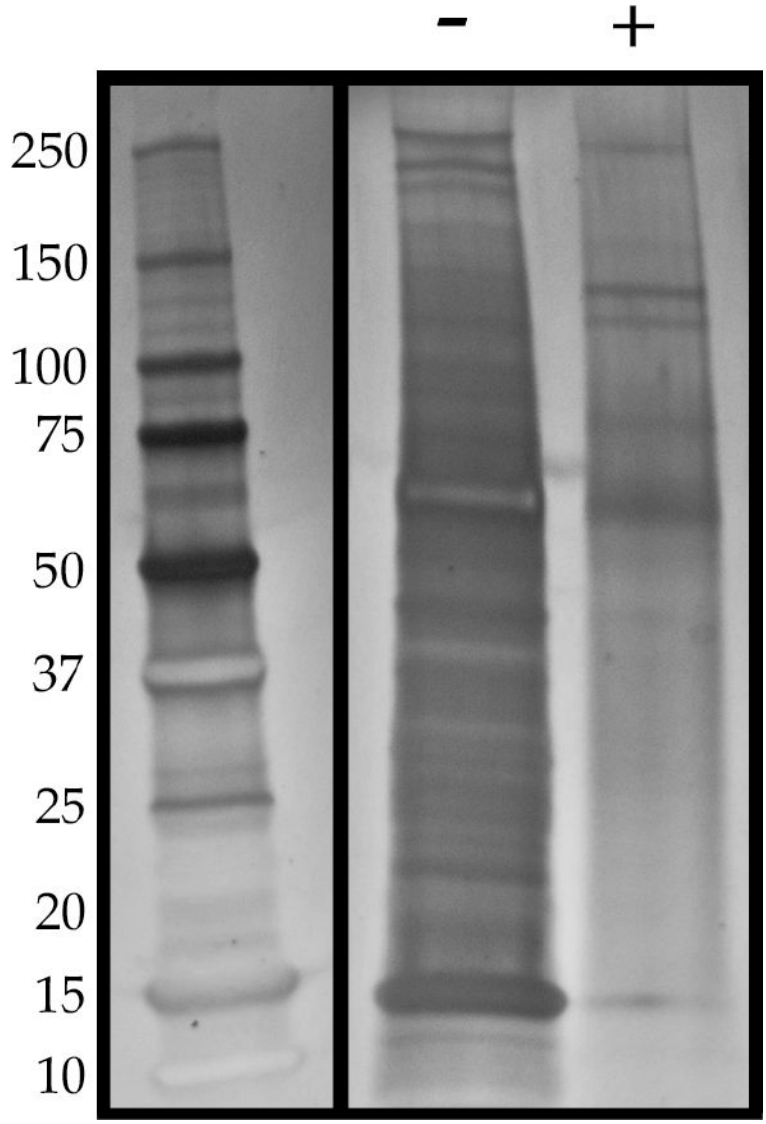

Figure 6.

Silver staining of total protein in native and decellularized human RPE/choroid. Silver staining shows overall protein loss in decellularized tissue ("+") compared to native tissue ("-"). The bands remaining in the decellularized choroid are primarily those with a larger molecular weight.

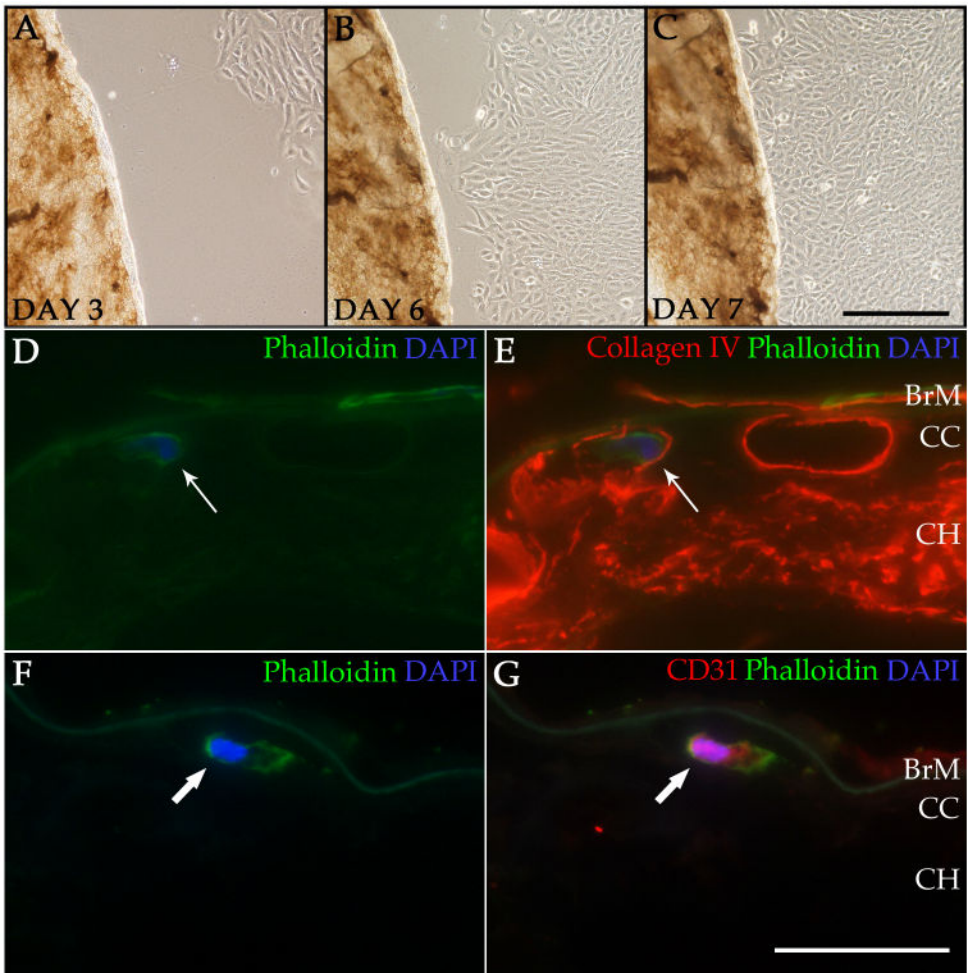

Figure 7.

Recellularization of the ECM scaffold with RF/6A cells or HRGECs. Brightfield images show RF/6A cells migrating toward the decellularized tissue during the recellularization process at day 3 (A)′ day 6 (B)′ and day 7 (C) in co-culture. Immunofluorescence images show phalloidin staining (green; D&E) of an RF/6A cell within a vascular tube of the choriocapillaris labeled with anti-collagen IV antibody (red; E). A CEC is also present on the surface of Bruch′s membrane. Phalloidin staining (green; F&G) and anti-CD31 immunolabeling (red; G) show a HRGEC within the choriocapillaris of a decellularized punch (F&G). Cell nuclei were counterstained with DAPI (blue; D-G). BrM = Bruch's membrane; CC = choriocapillaris; CH = choroid. Scale bar in C = 200 μm; scale bar in G = 50 μm

Table 1

Table of donor information.

Donor	Age	Sex	Eye	Ocular Disease	Cause of Death
1	78	Male	OD	Control	Acute Renal Failure
2	80	Female	OD	Control	Subarachnoid Hemorrhage
3	89	Female	OS	Control	Congestive Heart Failure
			OD	Control	
4	89	Male	OS	Control	Respiratory Failure
5	90	Female	OS	Control	Subdural Hematoma
6	93	Female	OD	Unknown	Respiratory Failure

Table 2

Top 50 full-length proteins present in the decellularized human RPE/choroid from th LC-MS/MS experiment.

Accession	Description	Score	Coverage	# Peptides	# PSM
P04004	Vitronectin	291.06	23.85	11	121
P02743	Serum amyloid P-component	190.78	33.63	9	105
P35555	Fibrillin-1	188.09	15.19	30	87
P13645	Keratin, type I cytoskeletal 10	202.92	29.28	14	78
P10909-4	Isoform 4 of Clusterin	184.67	21.39	6	77
P35908	Keratin, type II cytoskeletal 2 epidermal	197.46	32.39	14	77
P35625	Metalloproteinase inhibitor 3	180.65	47.39	9	65
Q07507	Dermatopontin	109.73	29.85	4	50
Q0IIN1	Keratin 77	90.79	5.02	3	41
D3DTX7	Collagen, type I, alpha 1, isoform CRA a	101.62	2.49	2	32
P02649	Apolipoprotein E	96.64	28.71	7	31
P08779	Keratin, type I cytoskeletal 16	75.30	23.68	8	28
P02533	Keratin, type I cytoskeletal 14	73.11	33.90	12	27
P48668	Keratin, type II cytoskeletal 6C	58.56	25.89	11	22
A0A024R035	Complement component 9, isoform CRA a	55.78	15.74	8	21
A0A087WTA8	Collagen alpha-2(I) chain	51.65	2.93	3	20
P13647	Keratin, type II cytoskeletal 5	48.09	19.83	10	17
P08493	Matrix Gla protein	37.12	11.65	2	17
O1523Ü	Laminin subunit alpha-5	40.95	4.38	12	16
P02760	Protein AMBP	44.46	19.03	4	15
P14543-2	Isoform 2 of Nidogen-1	34.46	10.41	9	15
A0A024R972	Laminin, gamma 1 (Formerly LAMB2), isoform CRA a	44.89	8.96	10	15
C8C504	Beta-globin	40.86	21.77	3	14
A0A024RAB6	Heparan sulfate proteoglycan 2 (Perlecan), isoform CRA b	37.48	4.39	13	14
P01024	Complement C3	39.28	5.35	6	13
V9HW34	Epididymis luminal protein 213	31.11	29.36	4	13
A0A087WZW8	Protein IGKV3-11	31.11	29.61	4	13

Accession	Description	Score	Coverage	# Peptides	# PSM
A0A087X130	Ig kappa chain C region	31.11	29.87	4	13
Q04695	Keratin, type I cytoskeletal 17	23.95	10.88	5	11
P55268	Laminin subunit beta-2	27.90	5.23	8	11
E7ENL6	Collagen alpha-3(VI) chain	26.70	5.53	11	11
E7ETP7	Elastin (Fragment)	31.35	16.67	3	9
Q9Y6C2	EMILIN-1	20.75	9.15	6	8
P68032	Actin, alpha cardiac muscle 1	16.43	12.73	3	6
P62736	Actin, aortic smooth muscle	16.43	12.73	3	6
P04004	Vitronectin	291.06	23.85	11	121
P02743	Serum amyloid P-component	190.78	33.63	9	105
P15924-2	Isoform DPII of Desmoplakin	13.17	2.42	5	6
S6BGE0	IgG H chain	9.88	15.00	3	5
Q03692	Collagen alpha-1 (X) chain	15.30	3.97	2	5
Q13103	Secreted phosphoprotein 24	14.73	17.06	4	5
P02042	Hemoglobin subunit delta	10.39	15.65	2	4
Q71U36-2	Isoform 2 of Tubulin alpha-1A chain	10.26	10.34	3	4
P14618	Pyruvate kinase PKM	11.11	6.59	3	4
P14618-2	Isoform M1 of Pyruvate kinase PKM	11.11	6.59	3	4
P13671	Complement component C6	11.49	2.68	2	4
F5GY80	Complement component C8 beta chain	11.72	4.35	2	4
B7Z550	Complement component 8, beta polypeptide, isoform CRA b	11.72	4.35	2	4
P59665	Neutrophil defensin 1	9.55	19.15	2	4
B3KVN2	Farnesyltransferase, CAAX box, alpha, isoform CRA c	8.94	10.09	2	4

Table 3

Mass spec data confirms retention of extracellular matrix and complement proteins in decellularized human RPE/choroid.

Extracellular Matrix Organization **rawP=8.83e-13; adjP=2.59e-10**		
Accession #	**Gene Symbol**	**Protein Name**
P14543-2	NID1	nidogen 1
P12110-3	COL6A2	collagen, type VI, alpha 2
A0A024R972	LAMC1	laminin, gamma 1
Q9Y6C2	EMILIN1	elastin microfibril interfacer 1
P08572	COL4A2	collagen, type IV, alpha 2
A0A024RAB6	HSPG2	heparan sufate proteoglycan 2
D3DTX7	COL1A1	collagen, type I, alpha 1
P55268	LAMB2	laminin, beta 2 (laminin S)
A0A087WTA8	COL1A2	collagen, type I, alpha 2
Q03692	COL10A1	collagen, type X, alpha 1
E7ETP7	ELN	Elastin
Q07507	DPT	Dermatopontin
E7ENL6	COL6A3	collagen, type VI, alpha 3
Extracellular Matrix Structural Constituent rawP=8.78e-14; adjP=4.04e-12		
Accession #	**Gene Symbol**	**Protein Name**
P12110-3	COL6A2	collagen, type VI, alpha 2
A0A024R972	LAMC1	laminin, gamma 1
Q9Y6C2	EMILIN1	elastin microfibril interfacer 1
P08572	COL4A2	collagen, type IV, alpha 2
P35555	FBN1	fibrillin 1
D3DTX7	COL1A1	collagen, type I, alpha 1
P08493	MGP	matrix Gla protein
Q6PID9	ACAN	Aggrecan
A0A087WTA8	COL1A2	collagen, type I, alpha 2
E7ETP7	ELN	Elastin
Membrane Attack Complex rawP=6.65e-12; adjP=1.12e-10		
Accession #	**Gene Symbol**	**Protein Name**
P07360	C8G	complement component 8, gamma
P13671	C6	complement component 6
P07357	C8A	complement component 8, alpha
Q9HDC9-2	C9	complement component 9
F5GY80	C8B	complement component 8, beta
Complement Activation rawP=2.00e-13; adP=1.65e-10		

Extracellular Matrix Organization rawP=8.83e-13; adjP=2.59e-10		
Accession #	**Gene Symbol**	**Protein Name**
Accession #	**Gene Symbol**	**Protein Name**
P07360	C8G	complement component 8, gamma
P01024	C3	complement component 3
A0A075B6N8	IGHG3	immunoglobulin heavy constant gamma 3
P10909-4	CLU	Clusterin
A0A087X130	IGKC	immunoglobulin kappa constant
P13671	C6	complement component 6
P07357	C8A	complement component 8, alpha
Q9HDC9-2	C9	complement component 9
F5GY80	C8B	complement component 8, beta